ISSN 1063-7788, Physics of Atomic Nuclei, 2020, Vol. 83, No. 11, pp. 1519–1528. © Pleiades Publishing, Ltd., 2020.

## RADIATION RESISTANCE OF MATERIALS AND EQUIPMENT

# Nanostructure Evolution of Oxide Dispersion Strengthened Steels under Fe Ion Irradiation at 350°C

**S. V. Rogozhkin[a,b,*], A. A. Khomich[a], A. A. Bogachev[a,b], A. A. Nikitin[a,b], V. V. Khoroshilov[a], T. V. Kulevoy[a], P. A. Fedin[a], K. E. Pryanishnikov[a], A. A. Lukyanchuk[a], O. A. Raznitsyn[a], A. S. Shutov[a], A. G. Zaluzhnyi[a,b], A. L. Vasiliev[c], and M. Yu. Presniakov[c]**

[a] *Alikhanov Institute for Theoretical and Experimental Physics, National Research Center "Kurchatov Institute", Moscow, 117218 Russia*

[b] *National Research Nuclear University MEPhI (Moscow Engineering Physics Institute), Moscow, 115409 Russia*

[c] *National Research Center "Kurchatov Institute", Moscow, 123182 Russia*

**e-mail: Sergey.Rogozhkin@itep.ru, SVRogozhkin@mephi.ru*

Received January 15, 2020; revised January 17, 2020; accepted July 24, 2020

**Abstract**—Improved mechanical properties of oxide dispersion strengthened (ODS) steels, the advanced materials for the reactor core, are due to the high density of uniformly distributed nanosized oxide inclusions. Transformation of the nanostructure of ODS steels under irradiation determines their stability during operation in the reactor conditions. In this work, three ODS steels are studied: Eurofer ODS, 10Cr ODS, and KP-3 ODS with different alloying systems. In these steels, the chromium content varies from 9 to 14 at %; such alloying elements as V, Ti, Al, W, and Mn are present in different proportions. The effect of irradiation with iron ions up to 3, 6, and 30 dpa at a temperature of 350°C was studied. The radiation-induced changes were analyzed by transmission electron microscopy and atom probe tomography. Although the sizes of oxide inclusions remained almost without change under irradiation, a decrease in their number density was observed in 10Cr ODS and KP-3 ODS steels, while the number density of oxides in Eurofer ODS steel did not change under the irradiation to 30 dpa. On the whole, the strengthening of the ODS steels due to inclusions during the irradiation to 30 dpa at 350°C changed insignificantly, which indicates their radiation resistance and their low propensity for low-temperature radiation strengthening and embrittlement.

**Keywords:** oxide, cluster, strengthening, atom probe tomography (APT), transmission electron microscopy (TEM), oxide dispersion strengthened (ODS) steel, irradiation, ions

**DOI:** 10.1134/S1063778820100208

## INTRODUCTION

Oxide dispersion strengthened (ODS) alloys and steels are developed as heat resistant materials for use in a variety of extreme conditions. In advanced nuclear power plants, these materials have to withstand temperatures up to 700°C and radiation doses up to 200 dpa [1, 2]. Advanced mechanical properties of ODS steels depend significantly on oxide nanoinclusions (particles and clusters) uniformly distributed across the matrix [3, 4]. At present, the stability of the nanostructure of ODS steels is studied with close attention [5, 6]. It was shown that irradiation at room temperature can lead to dissolution of large (>10 nm) oxides and nucleation of clusters enriched in Y, O, and V or Ti and small (<5 nm) oxide inclusions [7]. The increase in irradiation temperature to 300°C or higher stabilizes oxide inclusions in most cases [5]. Although the general mechanisms of the influence of irradiation on oxide inclusions are clear, there is no full understanding of these effects.

Note that a small number of certain alloying elements (Ti, Zr, V, Al, etc.) considerably reduces the size of oxide particles and increases their density in ODS steels (see, e.g. [8]). These structural modifications provide a significant improvement in the long-term strength of ODS materials at high temperatures as compared to conventional steels. However, it is not clear how important these nanostructure modifications are for their radiation resistance.

Currently, a wide range of ODS steels has been developed within national and/or research programs [9–12]. In this paper, three ODS steels with different alloying elements were studied. The reactor radiation load was simulated with heavy ions up to a dose of radiation damage of 30 dpa. The irradiation temperature of 350°C was chosen because of the importance of the analysis of low-temperature radiation embrittlement that determines the lower limit of the temperature interval of steel operation. The effect of the irradiation on the structural-phase state of steels was stud-

**Table 1.** Nominal chemical composition of the ODS steels under study, at %

| | Fe | Mo | Al | Ni | Mn | Cr | W | Y | O | Ti | V | C | N | Ar | Si |
|---|---|---|---|---|---|---|---|---|---|---|---|---|---|---|---|
| Eurofer ODS | 88.08 | — | — | 0.02 | 0.39 | 9.81 | 0.34 | 0.13 | 0.34 | — | 0.22 | 0.40 | 0.21 | — | 0.06 |
| 10Cr ODS | 86.90 | 0.57 | — | — | 0.50 | 10.64 | — | 0.17 | 0.17 | 0.29 | 0.11 | 0.60 | 0.02 | 0.01 | — |
| KP-3 ODS | 78.29 | — | 6.40 | — | — | 13.82 | 0.55 | 0.16 | 0.37 | 0.18 | — | 0.21 | — | — | — |

ied with transmission electron microscopy (TEM) and atomic probe tomography (APT).

## MATERIALS AND METHODS

In this paper, three steels are studied: Eurofer ODS, 10Cr ODS, and KP-3 ODS, whose chemical composition is presented in Table 1. These steels are distinguished by their content of chromium and certain alloying elements, such as Mn, W, Ti, and V. They were obtained by mechanical alloying of metal powders and $Y_2O_3$ powder. The materials under study were exposed to different thermomechanical finishing treatments. The KP-3 ODS steel from the Institute of Advanced Energy, Kyoto University (Japan), was enclosed in a mild steel capsule and degassed in the vacuum of $10^{-3}$ Torr at 400°C for 3 h. Hot extrusion was carried out at 1150°C to form a rod 25 mm in diameter which was subsequently annealed at 1150°C for an hour and cooled in the air. The production of 10Cr ODS steel from the Korea Atomic Energy Research Institute (Republic of Korea) was arranged in the following stages. The first stage was hot isostatic pressing at 1150°C for four hours at 100 MPa, then hot rolling at 1100°C, normalization at 1050°C for an hour with air cooling, and tempering at 780°C for an hour with air cooling. The Eurofer ODS steel from the Institute for Applied Materials, Karlsruhe Institute of Technology (Germany), was normalized at 1100°C for 30 min with water quenching and subsequent tempering at 750°C for two hours with air cooling.

Eurofer ODS and 10Cr ODS are 9–10% chromium structural steels for advanced fusion reactors [10, 11]. KP-3 ODS is high chromium ODS steel for advanced fission reactors with Al addition, with increased corrosion resistance when cooled by supercritical water or lead-bismuth coolant [12]. The yttrium content in steels is in the range of 0.13–0.17 at %, while the oxygen content varies widely: from 0.17 at % in 10Cr ODS to 0.37 at % in KP-3 ODS steel.

In this paper, the $Fe^{2+}$ ion beam accelerated to 5.6 MeV was used in the experiment in irradiation of ODS steel specimens [13]. According to SRIM calculations [14], the maximum number of defects generated in Fe at irradiation with the 5.6 MeV $Fe^{2+}$ beam is at a depth of about 1.4–1.5 μm (see Fig. 1). For the irradiation, disks 3 mm in diameter and 0.3 mm in thickness were cut. These specimens were mechanically polished to a thickness of 200 μm. The residual work hardening caused by mechanical thinning was removed from the irradiated surface by electrochemical polishing using a TenuPol-5 device for 30 s in a 10% solution of perchloric acid in ethanol. The voltage supplied to the specimen was selected according to the current density dependence curve. The surface roughness Ra of the specimen was controlled by atomic force microscopy before and after irradiation, and it was less than 20 nm for all specimens. The disk specimens were irradiated to the fluencies of $5 \times 10^{19}$, $1 \times 10^{20}$, and $5 \times 10^{20}$ $m^{-2}$ at 350°C. The calculated dose at the damage peak for these fluencies was ~5, 10, and 50 dpa, respectively. The dose at the depth of ~ 1 μm, where microscopic studies were performed, was 3, 6, and 30 dpa, respectively.

The chemical and phase composition of the steels was analyzed using TEM, electron diffraction (ED), and scanning transmission electron microscopy (STEM). A Titan 80-300 S/TEM microscope (Thermo Fisher Scientific, USA) with the acceleration voltage of 300 kV equipped with a high-angle dark field annular detector (HAADF, Fischione) was used to obtain Z-contrast photomicrographs. The qualitative and quantitative chemical analysis of specimens was performed with energy dispersive X-ray spectroscopy (EDXS).

The atomic-scale analysis of distribution of chemical elements in ODS steels was carried out with an atom probe tomograph with femtosecond laser assisted evaporation (APPLE-3D) developed at the Alikhanov Institute for Theoretical and Experimental Physics, National Research Center "Kurchatov Institute" [15]. Data was collected at the specimen temperature of 50 K in the laser evaporation mode with the wavelength of 515 nm, laser pulse duration of 300 fs, frequency of 25 kHz, and pulse energy of 0.1–1.2 μJ [16]. The pressure in the analytical chamber was ~$(5–7) \times 10^{-10}$ Torr.

The APT data analysis included the mass spectrum identification, as well as the reconstruction and analysis of three-dimensional distributions of chemical elements in the studied volumes using the KVANTM-3D software [17]. The maximum separation algorithm was used to search for and describe the detected nanoscale features [18, 19]. In this paper, the sum of such elements as Y, O, Ti, and W was used to search for clusters in the volumes studied. The procedure of finding optimal parameters for determining clusters was carried out separately for the initial and irradiated states.

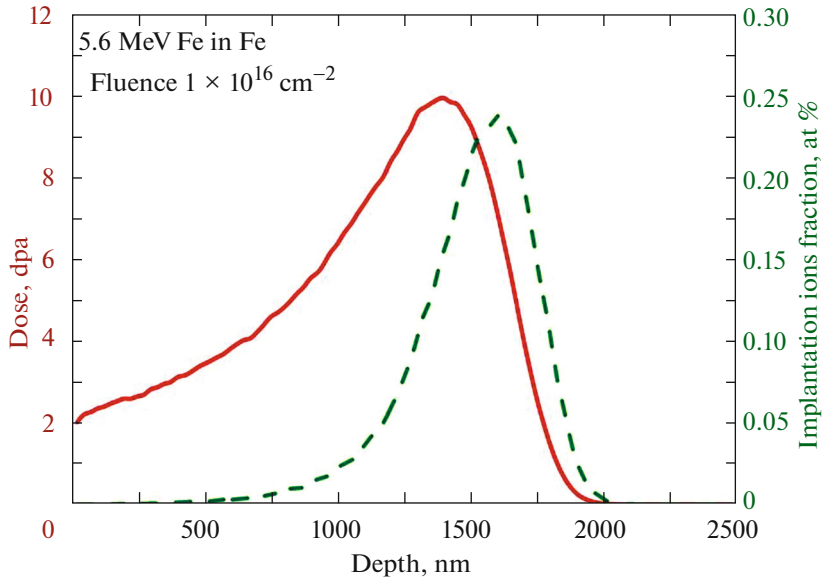


**Fig. 1.** Profiles of damage (solid line) and ion implantation (dotted line) in a pure iron specimen irradiated with the Fe ion beam with the energy of 5.6 MeV calculated by the SRIM2008 software package. Calculations are given for the ion fluency of $1 \times 10^{20}$ m$^{-2}$ and the threshold displacement energy of 40 eV.

Specimens for microscopic studies by the TEM and APT methods were produced by the focused ion beam (FIB) method using the $Ga^+$ ion beam in the HELIOS NanoLab 600 scanning electron-ion microscope (FEI, Holland) at the acceleration voltage of 5–30 kV. In order to reduce the thickness of the amorphous layer broken owing to the interaction with the ion beam, additional thinning was performed at the accelerating voltage of 2 kV. Thin cross-sectional specimens were produced for the TEM studies. Below, the results of the TEM analysis of the ion-irradiated specimens are presented for the depth of ~1 μm. For the APT analysis, a certain amount of material was extracted from the depth of 0.9–1 μm from the irradiated surface using the FIB methods, and attached to a solid base. Further, this specimen was polished with $Ga^+$ ions to obtain a needle-like shape with the radius of the tip apex less than 50 nm; the specimen was studied by the APT methods.

## ANALYSIS OF THE INITIAL STATE OF THE ODS STEELS

The microstructure of the ODS steels under study consists of typical ferrite grains of 0.3–2 μm in Eurofer ODS, 0.2–1.5 μm in 10Cr ODS, and 0.5–2 μm in KR-3 ODS [20]. The TEM images of the microstructure of the initial state of the examined ODS steels obtained in the scanning mode with the use of the high-angle annular dark-field detector (STEM-HAADF) are presented in Fig. 2.

The high number density of fine oxides was found in all ODS steels studied. The oxide sizes were 2–10 nm in Eurofer ODS, 1–6 nm in 10Cr ODS, and 2–5 nm in KR-3. The size distributions of oxides are shown in Fig. 3. Typical oxide sizes and number densities are shown in Table 2. It is known that large oxides in Eurofer ODS are stoichiometric $Y_2O_3$ particles with a small amount of Mn ($(Y_{1.8}Mn_{0.2})O_3$) [21]. Large oxides in 10Cr ODS are stoichiometric particles of $Y_2Ti_2O_7$ or $Y_2TiO_5$ [22]. It is considered that oxides in KR-3 ODS steel have the stoichiometry of $Y_4Al_2O_9$, $YAlO_3$, and $Y_3Al_5O_{12}$ [23, 24]. However, the chemical composition of inclusions smaller than 5 nm is difficult to detect using the TEM tools.

The APT analysis of the initial state of the ODS steels revealed nanoclusters (see Figs. 4 and 5). The largest number of clusters (~$10^{23}$ m$^{-3}$) was found in Eurofer ODS and 10Cr ODS steels (see Table 2). All detected clusters were enriched in Cr, Y, and O (see Table 3). Other alloying elements, such as Ti, V, and Al, also enrich clusters if they are included in the steel composition. Eurofer ODS steel that does not contain Ti has a significant amount of vanadium in the clusters. In 10Cr ODS steel that contains relatively close V and Ti concentrations, the clusters are mainly enriched in Ti (~6%). In KP-3 ODS steel containing ~30 times more Al than Ti (0.18%), the clusters are mainly enriched in Ti (~6%).

## STUDY OF IRRADIATED ODS STEELS

The results of the study of rearrangement of oxide inclusions in the ODS steels under Fe ion irradiation are presented in Fig. 6 and in Table 4. The TEM study

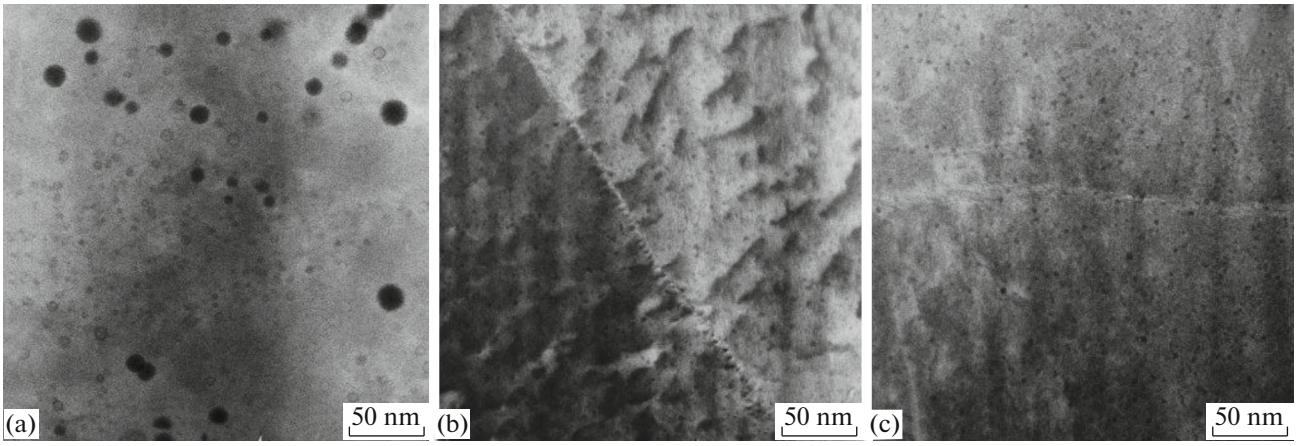


**Fig. 2.** STEM images of ODS steels: (a) Eurofer ODS; (b) 10Cr ODS; and (c) KP-3 ODS.

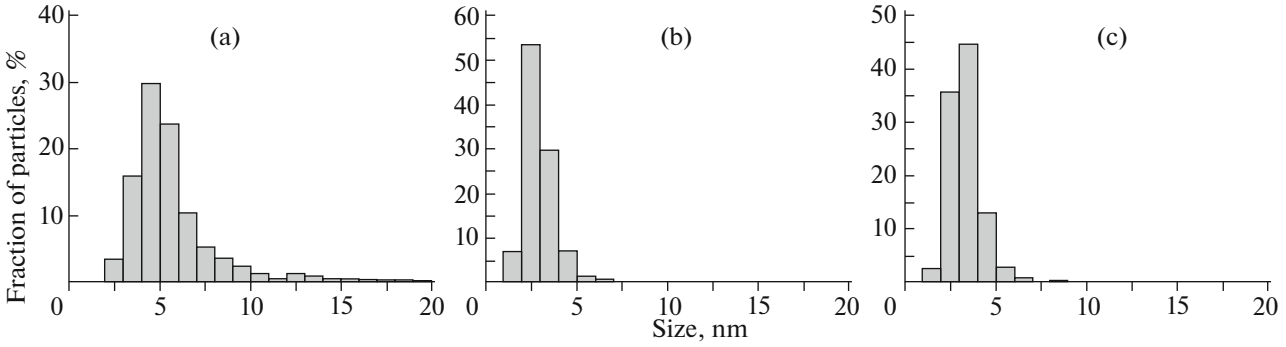


**Fig. 3.** Size distributions of oxide inclusions in steels: (a) Eurofer ODS; (b) 10Cr ODS; and (c) KP-3 ODS.

of irradiated Eurofer ODS steel revealed (see Fig. 6) the dissolution of large oxides (more than 10 nm) and formation of small oxide inclusions (less than 5 nm). This leads to a slight increase in the number density of oxides and a decrease in their mean size under the irradiation to 30 dpa.

In 10Cr ODS steel, the fraction of larger oxides increases at low doses of radiation, but this effect disappears at 30 dpa. KP-3 ODS steel demonstrates a stable size distribution at low irradiation doses, but at 30 dpa, the fractions of small (<2 nm) and large (>6 nm) oxide inclusions increase.

The APT showed that the initial state of Eurofer ODS steel contains clusters enriched in Y (up to 3 at %), O (up to 4 at %), Cr (up to 10 at %), V (up to 8 at %), and N (up to 4 at %), with the mean size of $3 \pm 1$ nm and the number density of $\sim 10^{23}$ m$^{-3}$. During the irradiation, with the growth of the damage dose, Cr, V, and N escape from the clusters (Fig. 7). The content of these elements in clusters is reduced to the average value in the material matrix. The atoms of these elements are replaced by iron atoms from the surrounding solid solution. At the same time, the mean Y concentration increases from 2.5 to 3.4 at %.

**Table 2.** Characteristic sizes and number densities of inclusions or clusters detected by the TEM and APT methods in the ODS steels

| | TEM analysis | | | APT analysis | | |
|---|---|---|---|---|---|---|
| | oxide inclusion type | inclusion size, nm | inclusion number density, $10^{22}$ m$^{-3}$ | cluster type | cluster size, nm | cluster number density, $10^{22}$ m$^{-3}$ |
| Eurofer ODS | Y–O | $6 \pm 2$ | 4 | Cr–Y–V–O | $3 \pm 1$ | $10 \pm 3$ |
| 10Cr ODS | Y–Ti–O | $3 \pm 1$ | 13 | Cr–Y–Ti–V–O | $4 \pm 1$ | $9 \pm 1$ |
| KP-3 ODS | Y–Al–O | $3 \pm 1$ | 9 | Cr–Y–Ti–Al–O | $4 \pm 1$ | $1.3 \pm 0.2$ |

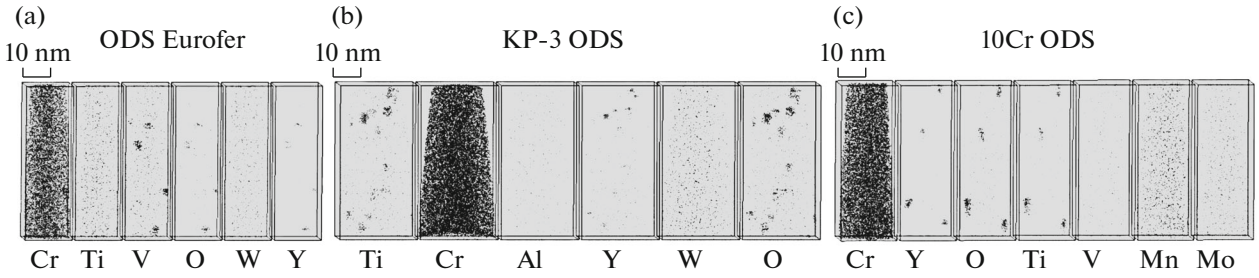


**Fig. 4.** Atom maps of the steels: (a) Eurofer ODS; (b) 10Cr ODS; and (c) KP-3.

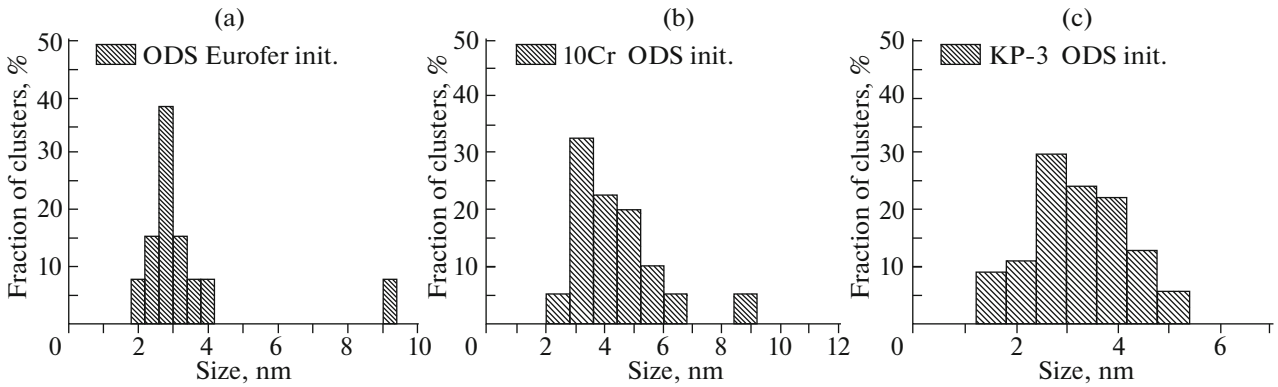


**Fig. 5.** Size distributions of clusters in the steels: (a) Eurofer ODS; (b) 10Cr ODS; and (c) KP-3 ODS.

The analysis of the initial state of 10Cr ODS steel by the APT methods showed that the material contained clusters enriched in Y (up to 3 at %), O (up to 7 at %), Cr (up to 4 at %), and Ti (up to 6 at %), with the mean size of $4 \pm 1$ nm and the number density of $\sim 10^{23}$ m$^{-3}$. Under the irradiation of 10Cr ODS steel, the Cr and V content in the clusters decreases to matrix values, while the Y concentration in the cluster composition slightly increases (from 3 to 4 at %) (Fig. 8).

In the initial state, KP-3 ODS steel contained clusters enriched in Y (up to 1 at %), O (up to 5 at %), Cr (up to 4 at %), Ti (up to 6 at %), and Al (up to 1 at %), with the mean size of $4 \pm 1$ nm and the number density of $\sim 10^{22}$ m$^{-3}$. Under the irradiation of this steel, with the growth of the damage dose, the mean size of oxide inclusions remained almost without changes. A slight decrease from 3 to 2 nm was observed under the irradiation to 30 dpa. The number density of inclusions decreased by half in comparison with the initial state under the irradiation up to 30 dpa. The local chemical analysis showed that, with the growth of the damage dose, the Cr content in the clusters decreased, while the Y and O content increased, and Al enrichment increased significantly, from 1 to 5 at % (Fig. 9). Under the irradiation to 30 dpa, clusters were not detected. This fact indicates that the cluster number density is much lower than $10^{21}$ m$^{-3}$.

## ANALYSIS OF CHANGES OF ODS STEEL HARDENING UNDER IRRADIATION

In order to analyze the changes in ODS steel hardening due to changes in the nanostructure, we use the dispersed barrier hardening model (DBH) model [25]. Within this model, each barrier type contributes to the hardening according to the Orowan formula:

$$\Delta\sigma_i = M_T \alpha_i \mu b \sqrt{N_i d_i}, \quad (1)$$

where $\alpha_i$ is the barrier strength, $M_T$ is the Taylor factor, $\mu$ is the share modulus, $b$ is the modulus of the Burgers vector, and $N_i$ and $d_i$ are the number density

**Table 3.** Chemical composition of clusters in the ODS steels under study, at %

| | Cr | Al | Y | O | Ti | V | N |
|---|---|---|---|---|---|---|---|
| Eurofer ODS | $10 \pm 5$ | — | $3 \pm 1$ | $4 \pm 2$ | — | $8 \pm 4$ | $4 \pm 2$ |
| 10Cr ODS | $4 \pm 2$ | — | $3 \pm 2$ | $7 \pm 4$ | $6 \pm 3$ | $0.8 \pm 0.4$ | — |
| KP-3 ODS | $4 \pm 2$ | $0.8 \pm 0.4$ | $1.3 \pm 0.7$ | $4 \pm 2$ | $6 \pm 3$ | — | — |

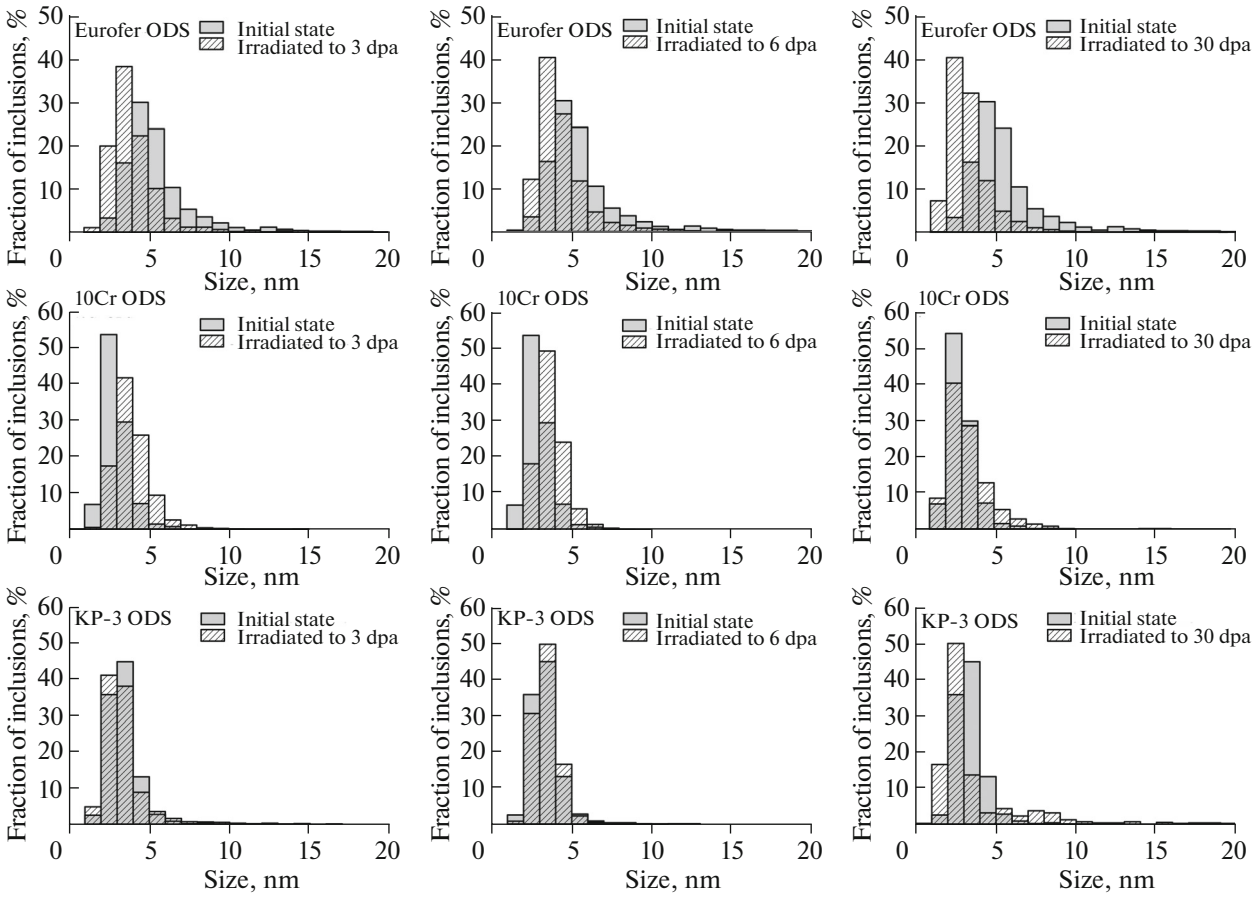


**Fig. 6.** Size distributions of oxides in the irradiated steels Eurofer ODS, 10Cr ODS, and KP-3 as compared with the size distributions in the initial state.

and the mean size of this barrier type. We take the value of 0.63 obtained from the in situ TEM tensile testing as the barrier size for oxide inclusions [26] and the value of 0.1 as the barrier strength for nanoclusters [27].

The results of calculation of the hardening caused by the oxide inclusions and clusters detected within the DBH model are presented in Table 5.

The estimates based on the DBH model show that the hardening contribution from the oxides inclusions and clusters in ODS steels does not increase under irradiation, and that there is a tendency toward the hardening reduction. In general, this indicates that the studied ODS steels are quite stable at 350°C up to doses of ~30 dpa.

The results show significant benefits in using the advanced ODS steels not only because of their high heat resistance but also owing to their low propensity

**Table 4.** Characteristic sizes and number densities of oxide inclusions detected by TEM in ODS steels under the irradiation with $Fe^{2+}$ with the energy of 5.6 MeV at 350°C

| TEM | | Eurofer ODS | 10Cr ODS | KP-3 ODS |
|---|---|---|---|---|
| Initial | Sizes, nm | 6 ± 2 | 3 ± 1 | 3 ± 1 |
| | Density, $10^{22}$ m$^{-3}$ | 4 | 13 | 9 |
| Irradiated to 3 dpa | Sizes, nm | 4 ± 1 | 4 ± 1 | 3 ± 1 |
| | Density, $10^{22}$ m$^{-3}$ | 4 | 7 | 9 |
| Irradiated to 6 dpa | Sizes, nm | 4 ± 1 | 4 ± 1 | 3 ± 1 |
| | Density, $10^{22}$ m$^{-3}$ | 5 | 9 | 8 |
| Irradiated to 30 dpa | Sizes, nm | 3 ± 1 | 3 ± 1 | 2 ± 2 |
| | Density, $10^{22}$ m$^{-3}$ | 5 | 4 | 5 |

**Table 5.** Characteristic sizes and number densities of clusters detected by APT in ODS steels under the irradiation with $Fe^{2+}$ with the energy of 5.6 MeV at 350°C

| TEM | | Eurofer ODS | 10Cr ODS | KP-3 ODS |
|---|---|---|---|---|
| Initial | Sizes, nm | 3 ± 1 | 4 ± 1 | 4 ± 1 |
| | Density, $10^{22}$ m$^{-3}$ | 10 ± 3 | 9 ± 1 | 13 ± 2 |
| Irradiated to 3 dpa | Sizes, nm | 4 ± 1 | 4 ± 1 | 3 ± 1 |
| | Density, $10^{22}$ m$^{-3}$ | 12 ± 2 | 11 ± 5 | 3 ± 1 |
| Irradiated to 6 dpa | Sizes, nm | — | 3 ± 1 | 3 ± 2 |
| | Density, $10^{22}$ m$^{-3}$ | — | 6 ± 2 | 8 ± 3 |
| Irradiated to 30 dpa | Sizes, nm | 3 ± 1 | 2 ± 1 | 0 |
| | Density, $10^{22}$ m$^{-3}$ | 7 ± 2 | 4 ± 2 | 0 |

for low-temperature radiation strengthening and embrittlement.

## CONCLUSIONS

The study of radiation resistance of the steels Eurofer ODS, 10Cr ODS, and KP-3 ODS with different alloying systems was carried out using heavy ion irradiation providing high damage rate. The materials were irradiated at 350°C with $Fe^{2+}$ ions. The integrally achieved fluencies were $5 \times 10^{19}$, $1 \times 10^{20}$, and $5 \times 10^{20}$ m$^{-2}$, which corresponded to the damage doses of 3, 6, and 30 dpa, respectively, in the analyzed area of materials.

A comprehensive study of the microstructure and local chemical composition of materials has been carried out using the TEM and APT methods. The microstructure of the studied steels is α-ferrite containing round and rectangular grains with the sizes of ~0.2–2 μm. Inside the ODS steel grains, there are oxide inclusions with the size of ~6 nm and the number density of ~$4 \times 10^{22}$ m$^{-3}$ in Eurofer ODS, 3 nm and $13 \times 10^{22}$ m$^{-3}$ in 10Cr ODS, and 3 nm and $9 \times 10^{22}$ m$^{-3}$ in KP-3 ODS, respectively. Large oxides with the sizes of 40–100 nm and the number density of $10^{18}$ m$^{-3}$ are also found in the Eurofer ODS steel. The local nanochemical APT analysis shows the presence of high density of clusters with the sizes of 2–5 nm and the density of ~$10^{23}$ m$^{-3}$ in Eurofer ODS and 10Cr ODS steels, and the density of ~$10^{22}$ m$^{-3}$ in KP-3 ODS steel. In all the steels studied, the clusters are enriched in Cr, Y, and O atoms. In Eurofer ODS steel, clusters also contain V atoms; there are Ti atoms in clusters in 10Cr ODS and KP-3 ODS steels, while clusters in KP-3 ODS steel also contains Al atoms.

In the Eurofer ODS steel, under irradiation to the dose of 3 dpa, the mean size is reduced from 6 to 4 nm. Further irradiation has practically no effect on the mean cluster size. At the same time, the irradiation does not affect the number density of inclusions, which remains at the level of $4 \times 10^{22}$ m$^{-3}$. The studies of the distribution of atoms in the material show that, because of the irradiation, clusters remain in the material structure with almost no changes in their sizes;

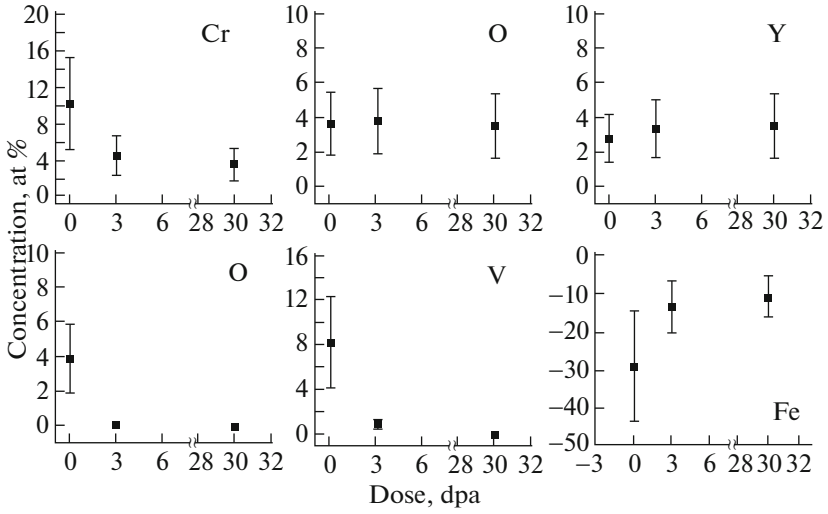


**Fig. 7.** Enrichment of clusters in the Eurofer ODS steel under different doses of irradiation.

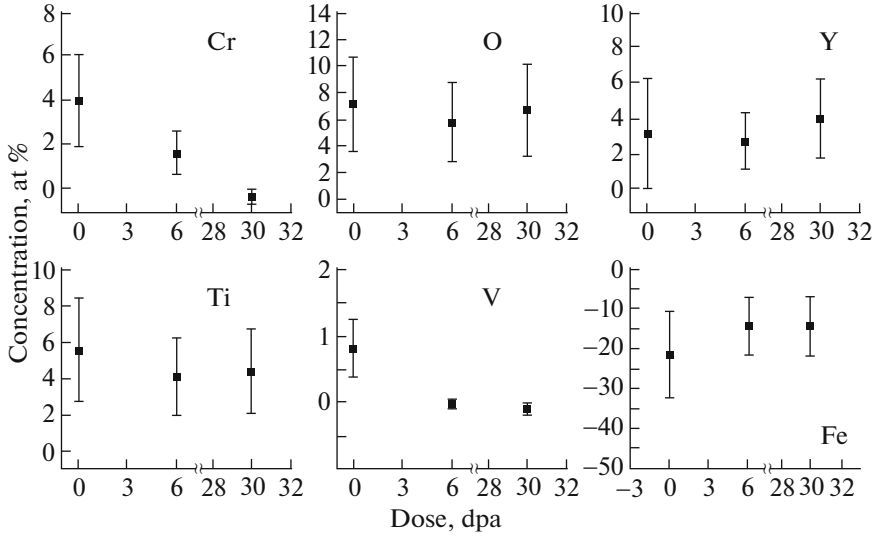


**Fig. 8.** Enrichment of clusters in the 10Cr ODS steel under different doses of irradiation.

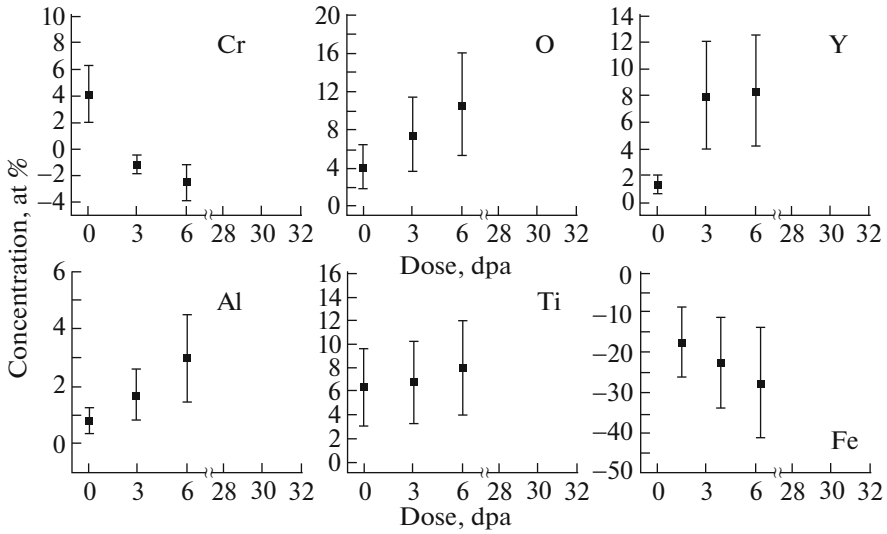


**Fig. 9.** Enrichment of clusters in the KP-3 ODS steel under different doses of irradiation.

when the irradiation dose increases, the number density decreases, and the chemical composition changes. In the Eurofer ODS steel, under irradiation with increasing damage dose, Cr, V, and N escape from the clusters. The content of these chemical elements in clusters is reduced to their mean matrix concentration levels, while the mean Y concentration increases from 2.5 to 3.4 at %.

In the 10Cr ODS steel, the mean size of oxide inclusions does not change with the growth of the damage dose and remains within 2–5 nm. At the dose of 30 dpa, there is also a nearly threefold decrease in the number density of inclusions to $3 \times 10^{22}$ $m^{-3}$. According to the APT analysis, in the 10Cr ODS steel, the Cr and V content in the clusters declines to matrix values, while the share of Y in clusters slightly increases (from 3 to 4 at %).

Under irradiation, with the increase in the damage dose, the mean size of oxide inclusions in KP-3 ODS steel does not change, which is similar to the 10Cr ODS steel. A slight decrease from 3 to 2 nm is observed when the steel is irradiated to 30 dpa. Under irradiation to 30 dpa, the number density of inclusions decreases by half as compared with the initial state. The local chemical analysis shows that the Cr content in the clusters decreases with the growth of the damaging dose, while the Y and O contents increase, and the enrichment in Al increases significantly from 1 to 5 at %. In the state under irradiation to 30 dpa, clusters are not observed. The distribution of chemical elements in the

**Table 6.** Calculations of hardening within the DBH model due to oxide inclusions and clusters of the ODS steels

| | | Hardening TEM | Hardening APT | Total hardening |
|---|---|---|---|---|
| Eurofer ODS | Initial | 0.6 ± 0.1 | 0.11 ± 0.02 | 0.6 ± 0.1 |
| | Irradiated to 3 dpa | 0.51 ± 0.06 | 0.14 ± 0.02 | 0.53 ± 0.06 |
| | Irradiated to 6 dpa | 0.57 ± 0.07 | 0 | 0.57 ± 0.07 |
| | Irradiated to 30 dpa | 0.49 ± 0.08 | 0.09 ± 0.01 | 0.50 ± 0.08 |
| 10Cr ODS | Initial | 0.8 ± 0.1 | 0.12 ± 0.01 | 0.8 ± 0.1 |
| | Irradiated to 3 dpa | 0.67 ± 0.08 | 0 | 0.67 ± 0.08 |
| | Irradiated to 6 dpa | 0.76 ± 0.09 | 0.09 ± 0.01 | 0.77 ± 0.09 |
| | Irradiated to 30 dpa | 0.44 ± 0.07 | 0.06 ± 0.01 | 0.44 ± 0.07 |
| KP-3 ODS | Initial | 0.7 ± 0.1 | 0.15 ± 0.02 | 0.7 ± 0.1 |
| | Irradiated to 3 dpa | 0.7 ± 0.1 | 0.06 ± 0.01 | 0.7 ± 0.1 |
| | Irradiated to 6 dpa | 0.6 ± 0.1 | 0.10 ± 0.03 | 0.6 ± 0.1 |
| | Irradiated to 30 dpa | 0.4 ± 0.2 | 0 | 0.4 ± 0.2 |

investigated specimens is homogeneous. This fact indicates that the number density of clusters is much smaller than $10^{21}$ $m^{-3}$.

The estimates of the contributions of oxide inclusions and clusters based on the DBH model show that the hardening contribution from the main barriers of ODS steels does not increase under irradiation. The results show that the studied ODS steels are quite stable at 350°C up to doses of ~30 dpa.

The results show significant advantages of using ODS steels not only because of their high heat resistance but also owing to their low propensity for low-temperature radiation strengthening and embrittlement.

## ACKNOWLEDGMENTS

We are grateful to Dr. P. Vladimirov at the Karlsruhe Institute of Technology (Germany), Professor A. Kimura at the University of Kyoto (Japan), and Dr. T.K. Kim (Republic of Korea) at the Korea Atomic Energy Research Institute for providing ODS steel specimens.

## FUNDING

This work was supported by the Russian Science Foundation, project no. 17-19-01696. The equipment of the KAMIKS Shared Access Center (http://kamiks.itep.ru/) at the Alikhanov Institute for Theoretical and Experimental Physics, National Research Center "Kurchatov Institute," was used for the specimen irradiation and ATP analysis. The equipment of the NANOZOND Resource Center, National Research Center "Kurchatov Institute" (http://www.rc.nrcki.ru/pages/main/nanozond/), was used for specimen preparation by the FIB methods and analysis by the TEM methods.

## CONFLICT OF INTEREST

The authors declare that they have no conflicts of interest.

## REFERENCES

1. P. Yvon and F. Carre, J. Nucl. Mater. **385**, 217 (2009).
2. R. L. Klueh, J. P. Shingledecker, R. W. Swindeman, and D. T. Hoelzer, J. Nucl. Mater. **341**, 103 (2005).
3. S. Ukai, T. Okuda, M. Fujiwara, T. Kobayashi, S. Mizuta, and H. Nakashima, J. Nucl. Sci. Technol. **39**, 872 (2002).
4. D. T. Hoelzer, J. Bentley, M. A. Sokolov, M. K. Miller, G. R. Odette, and M. J. Alinger, J. Nucl. Mater. **367–370**, 166 (2007).
5. J. P. Wharry, M. J. Swenson, and K. H. Yano, J. Nucl. Mater. **486**, 11 (2017).
6. X. Liu, Y. Miao, Y. Wu, S. A. Maloy, and J. F. Stubbins, Scr. Mater. **138**, 57 (2017).
7. S. Rogozhkin, A. Bogachev, O. Korchuganova, A. Nikitin, N. Orlov, A. Aleev, A. Zaluzhnyi, M. Kozodaev, T. Kulevoy, B. Chalykh, R. Lindau, A. Moslang, P. Vladimirov, M. Klimenkov, M. Heilmaier, J. Wagner, and S. Seils, Nucl. Mater. Energy **9**, 66 (2016).
8. S. Ukai and M. Fujiwara, J. Nucl. Mater. **307–311,** 749 (2002).
9. Y. Carlan, J.-L. Bechade, P. Dubuisson, J.-L. Seran, P. Billot, A. Bougault, T. Cozzika, S. Doriot, D. Hamon, J. Henry, M. Ratti, N. Lochet, D. Nunes, P. Olier, T. Leblond, and M. H. Mathon, J. Nucl. Mater. **386–388,** 430 (2009).
10. R. Mateus, P. A. Carvalho, D. Nunes, L. C. Alves, N. Franco, J. B. Correia, and E. Alves, Fusion Eng. Des. **86**, 2386 (2011).
11. Y. H. Jeong, W. J. Kim, D. J. Kim, J. Jang, S. H. Kang, Y.-B. Chun, and T. K. Kim, Proc. Eng. **86**, 1 (2014).
12. A. Kimura, H.-S. Cho, N. Toda, R. Kasada, K. Yutani, H. Kishimoto, N. Iwata, S. Ukai, and M. Fujiwara, J. Nucl. Sci. Technol. **44**, 323 (2007).
13. S. V. Rogozhkin, A. A. Nikitin, A. A. Khomich, N. A. Iskandarov, V. V. Khoroshilov, A. A. Bogachev,

A. A. Lukyanchuk, O. A. Raznitsyn, A. S. Shutov, P. A. Fedin, R. P. Kuibeda, T. V. Kulevoy, A. L. Vasiliev, M. Yu. Presniakov, K. S. Kravchuk, and A. S. Useinov, Phys. At. Nucl. **82**, 1239 (2019); Yad Fiz. Inzhin. **9**, 245 (2018).

14. www.srim.org/.

15. S. V. Rogozhkin, A. A. Aleev, A. A. Luk'yanchuk, A. S. Shutov, O. A. Raznitsyn, and S. E. Kirillov, Instrum. Exp. Tech. **60**, 428 (2017).

16. O. A. Raznitsyn, A. A. Lukyanchuk, A. S. Shutov, S. V. Rogozhkin, and A. A. Aleev, J. Anal. Chem. **72**, 1404 (2017).

17. A. A. Aleev, S. V. Rogozhkin, A. A. Lukyanchuk, A. S. Shutov, O. A. Raznitsyn, A. A. Nikitin, N. A. Iskandarov, O. A. Korchuganova, and S. E. Kirillov, State Registration Certificate of Computer Program No. 2018661876 (2018). https://www1.fips.ru/ofpstorage/Doc/IZPM/RUNWC1/000/000/002/702/112/%D0%98%D0%97-02702112-00001/document.pdf.

18. M. K. Miller, *Atom Probe Tomography: Analysis at the Atomic Level* (Kluwer Academic, New York, 2000).

19. A. Cerezo and L. Davin, Surf. Interface Anal. **39**, 184 (2007).

20. S. V. Rogozhkin, A. A. Khomich, A. A. Bogachev, A. A. Nikitin, A. A. Lukyanchuk, O. A. Raznitsyn, A. S. Shutov, A. L. Vasiliev, and M. Yu. Presniakov, Phys. At. Nucl. **83**, 1425 (2020).

21. M. Klimenkov, R. Lindau, and A. Möslang, J. Nucl. Mater. **386–388,** 553 (2009).

22. D. Bhattacharyya, P. Dickerson, G. R. Odette, S. A. Maloy, A. Misra, and M. Nastsi, Philos. Mag. **92**, 2089 (2012).

23. L. Hsiung, M. Fluss, S. Tumey, J. Kuntz, B. El-Dasher, M. Wall, B. Choi, A. Kimura, F. Willaime, and Y. Serruys, J. Nucl. Mater. **409**, 72 (2011).

24. S. Xu, Z. Zhou, H. Jia, and Z. Yao, Steel Res. Int. **90**, 1800594 (2018).

25. G. E. Lucas, J. Nucl. Mater. **206**, 287 (1993).

26. E. Gil, N. Ordás, C. García-Rosales, and I. Iturriza, Fusion Eng. Des. **98–99,** 1973 (2015).

27. M. J. Swenson, C. K. Dolph, and J. P. Wharry, J. Nucl. Mater. **479**, 426 (2016).

*Translated by N. Semenova*